VERIFICATION OF CANONICAL PROFILES AND SEMI EMPIRICAL TRANSPORT MODELS AGAINST JT-60U PLASMAS

Yu.N. Dnestrovskij, S.E. Lysenko, K.N. Tarasyan
Russian Research Center 'Kurchatov Institute', Moscow 123182, Russian Federation

A.R. Polevoi[1], T. Takizuka, H. Shirai, M. Kikuchi
Naka Fusion Research Establishment, Japan Atomic Energy Research Institute,
Naka-machi, Naka-gun, Ibaraki-ken, 311-0193, Japan

Abstract

The canonical profiles transport model (CPTM) and the semi empirical transport model (SETM) are verified against JT-60U plasmas. The simulations were carried out by 1.5 transport code ASTRA, comprising the particles transport, and the electron and ion heat transport.

1. DESCRIPTION OF THE INTERNAL THERMAL BARRIER (ITB) BY THE CPTM

The appearance of the ITB in JT-60U was described in [1,2]. To obtain the ITB it is necessary to deposit a high and peaked heating power and to suppress the MHD activity by creation of q(0)>1. **The set of transport equations** consists of the equations for the electron and ion temperatures, T_e, T_i, the plasma density n, and the poloidal magnetic field expressed through $\mu=1/q$. The main part of the heat flux has the following form [3]:

$$\Gamma_k^{PC} = -n\chi_k^{PC}(\partial T_k/\partial r - T_{kc}' T_{kc}^{-1} T_k)F_k, \quad F_k(z_{pk}) = \exp(-0.5 z_{pk}^2 z_{0k}^{-2}), \quad (k=e, i) \qquad (1)$$

The particle flux Γ_n has the similar structure. The transport coefficients χ_k^{PC} and others were defined in [3]. The ITB is described by the very nonlinear 'forgetting factor' $F_k(z_{pk})$. Here $z_{pk}=a^2/r\times\partial/\partial r[\ln(p_k/p_{kc})]$ is the dimensionless deviation of the real pressure profile $p_k(r)$ from the canonical one $p_{kc}(r)$. For the canonical profiles $T_{kc}(r)$, and $p_{kc}(r)$ we use familiar Kadomtsev's expressions. The critical deviation profile $z_{0k}(r)$ was prescribed by the piece-wise linear function [3]:

$z_{0k}(r)=\alpha_{0k}$ at $0<r<r_1$, $z_{0k}(r)=\alpha_{0k}+(z_0^k-\alpha_{0k})(r_0-r_1)^{-1}(r-r_1)$ at $(r_1<r<r_2)$, and $z_{0k}(r)=z_0^k$ at $r_2<r<a$.
Here $z_{0e}(0)=\alpha_{0e}=4$-5, $z_{0i}(0)=\alpha_{0i}=1.5$-$2$, $z_0^k=7$-9, $r_1=0.45a$, $r_2=0.8a$.

The criterion of bifurcation follows from (1) and has the form $F_k<<1$ or $|z_{pk}|>z_{0k}$ or

$$|a^2 r^{-1}(p_k'/p_k - p_{kc}'/p_{kc})| > z_{0k} \qquad (2)$$

at some point in the gradient zone. To make the criterion (2) clearer, we introduce the parametrical expression for the power density profile deposited to ions:

$$P^i(x)=P_0, \quad (0 < x < x_0) \qquad P^i(x)=P_0 \exp(-\eta(x-x_0)) \qquad (x_0<x<1), \quad x=r/a \qquad (3)$$

The profiles (3) with x_0 =0.3, η=5, 10, 25 are shown in Fig. 1 by solid lines. The dashed lines correspond to the experimental profiles 'A' and 'B' [1]. The calculations of the threshold power P_{thr} were carried out for the shot #E27302 (a=0.74 m, R=3.15 m, B=4.28 T, I=2.47 MA, $n=2.7\times10^{19}$ m^{-3}). Figure 2 shows the dependence of the P_{thr} on the e-fold parameter η for different values of flat-top parameter x_0. At fixed x_0 and η rising, the threshold rapidly diminishes to the level of 3 MW. From the other hand, if η is less than some critical value η_{cr} ($\eta<\eta_{cr}$), the value of P_{thr} becomes indefinitely

---

[1] Permanent affiliation RRC 'Kurchatov Institute'

large. Figure 3 shows the dependence of η_{cr} on x_0. This curve divides the (x_0, η_{cr}) plane into two parts. The ITB can appear only for points disposed above the drawn curve:

$$x<x_{0cr},\ \eta>\eta_{cr},\ \text{and}\ P^i_{tot}>P_{thr}(\eta, x_0) \qquad (4)$$

Small regions 'A', 'B' and 'C' (#E26402) in Fig. 3 correspond to the different profiles of deposited power from [1, 2]. It follows from Fig. 3 that the ITB can appear only for the 'A' and 'C' types of profiles, that corresponds to the experiments [1, 2].

Simulation of JT-60U shots with ITB was carried out by the model (1). Figure 4 presents $T_i(r)$ profiles at different time instants and appearance of ITB for shot #E27302 (P^i_{NB}=9 MW, P^e_{NB}= 3 MW). Note that the 'foot point' of ITB moves from r/a~0.45 to r/a=0.65. A good correlation between the calculations and experimental data is seen.

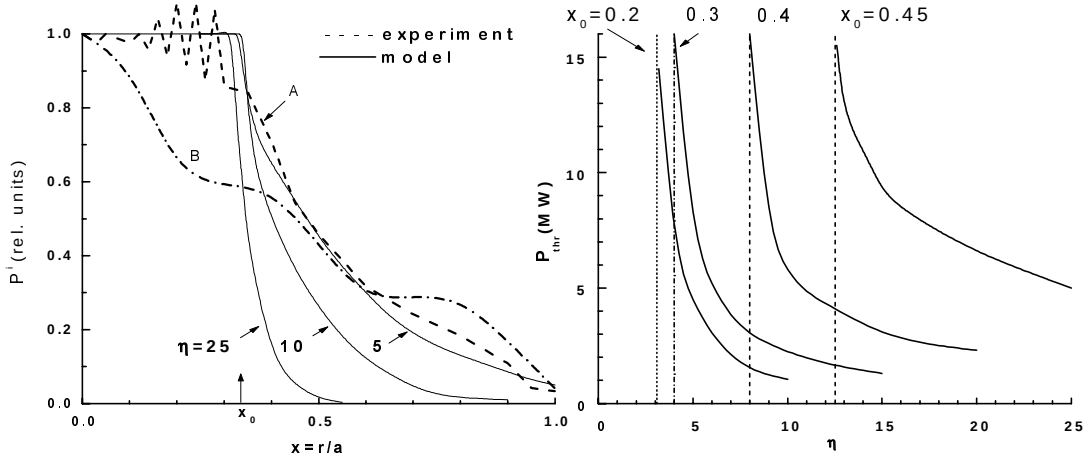

FIG. 1. Experimental (A and B) and model profiles of NBI power deposited to ions.

FIG. 2. Threshold power for ITB formation at various e-fold parameters from Fig. 1 and Eq. 3

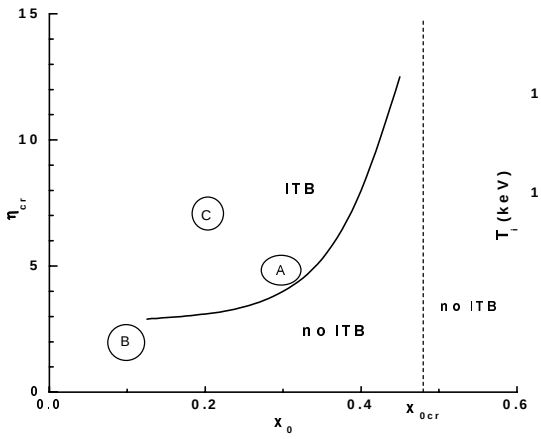

FIG. 3. Regions with and without ITB at various e-fold and flat-top parameters of deposited NBI power. Curves A, B and C correspond to experimental shots.

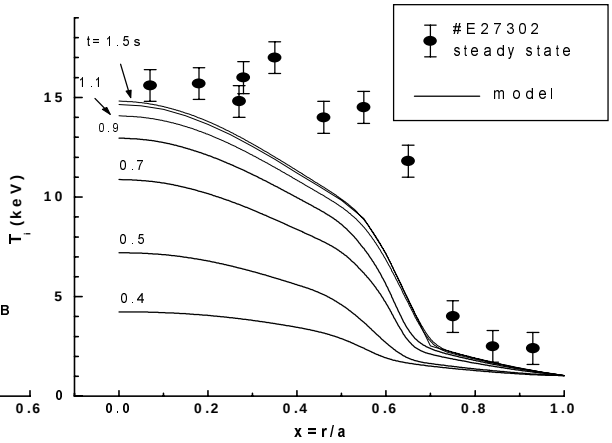

FIG. 4. Time evolution of calculated ion temperature profiles (solid lines). Points are the steady state experimental profile

2. SIMULATION OF JT-60U PLASMAS WITH THE SEMI EMPIRICAL TRANSPORT MODEL

The SETM includes self consistent simulations of the heat and particle transport with the convective term in the heat transport equations. The model comprises anomalous electron and ion transport coefficients. The T-11 model transport coefficients [4] with Ohkawa type parametric dependence $D_e,\chi_e \sim (c/\omega_p)^2$ are used for the anomalous electron heat conductivity and particle diffusivity. For the anomalous ion heat diffusivity we used the expression of the ref. [8]: $\chi_i \sim d\ v_i\ \beta^{0.5}$, where d is the Debye radius, v_i is the ion thermal velocity. We modified the SET model to fit the JT-60U experimental data in the reversed shear case, replacing the current profile dependence $f \sim (q-q_0)^3$ used in pervious analysis [5] by $f \sim (q-q_{min})^3$, where q_{min} is a minimum of the safety factor q. The final form of the coefficients is as follows:

$$\chi_i = T_e^{1/2}\ T_i(0)\ B^{-1}\ F, \qquad (5)$$

where

$$F = 0.42\ (Z_{eff} A_i)^{-1/2} \langle n \rangle\ n^{-1} f\ (1-\exp(-f\ Y))^{-1},$$

$$f = 0.125\ (q-q_{min})^3,$$

Y is a function of the dimensionless combination of the elecrton Larmor radius ρ_e, Debye radius d and β. $Y = 2.5\ T_i Z_{eff}^{-1} a^{0.25} n^{0.125} \sim (d/\rho_e)^2 \beta^{1.125} (a/\rho_e)^{0.25}$ [8]. Here we use the following units: T_e, T_i (keV), B (T), n, $\langle n \rangle$ ($10^{19} m^{-3}$), a (m).

We also supposed that radial transport of the fast particles density n_f is negligible in comparison with the anomalous diffusion of the thermalised particles D_e [4]. So to keep quasi neutrality and ambipolarity we reduce the particle diffusion the following way:

$$D_e\ n_e' \rightarrow D_e\ (n_e' - n_f'\ T_i\ T_e^{-1}\ (Z_{eff} - n_f/n_e)^{-1}. \qquad (6)$$

This correction could play role for powerful NBI into the plasma of low density during the transient phase of the JT-60U high-β_p discharges.

The SET model was applied to the analysis of the JT-60U L-mode and H-mode discharges in the deuterium plasma with the NBI heating. The simulations were carried out using the ASTRA-code [7] with the self consistent simulations of plasma equilibrium, poloidal flux evolution, CX-neutral distribution and NBI [6]. The model is not completely predictive since it uses the boundary conditions and impurity radiation from the experiment. These values strongly vary in different experiments. Our simulations include also a 'hidden parameter'. The cold neutral flux from the boundary is fitted to provide the experimental time evolution of the average plasma density. In some discharges CX losses of fast ions, caused by this flux could have a noticeable impact on the plasma heating. But it is poorly measurable in the experiments. That usually increases the uncertainty of the experimental data interpretation.

We analyzed the L-mode discharges with the plasma current in the range of I_p = 1 - 2.25 MA, plasma volume V = 62 - 84 m^3, the input NBI power P_{NB} = 5.4- 13.4 MW, B=2.1 - 4T, $\langle n \rangle$ = 0.9 - $2.6\times10^{19} m^{-3}$ and high performance discharges with I_p = 0.8-1.5 MA, B = 2.1 - 3.5 T, V = 52-62 m^3, $\langle n \rangle$ = 2.5 - $3.5\times10^{19} m^{-3}$, P_{NB} = 15 - 27 MW. The comparison of the SETM prediction for the total energy content and chord integrated density evolution reveals satisfactory agreement with the experimental data. The SET model reproduces also the experimental temperatures and density radial distributions (FIG.5). **Thus, SETM satisfactory describes particle and heat transport in the JT-60U L-mode and H-mode discharges with the same parametric dependencies for all transport coefficients.**

The SET model gives less values of the ion heat conductivity near the magnetic axis than the neoclassical theory predicts. In the zone of good confinement, where $f Y << 1$ ($q \sim q_{min}$ or low T_i), $\chi_i \sim T_e^{1/2}$ and degrades fast out of this zone as $\chi_i \sim T_e^{1/2} T_i(0)\ (q-q_{min})^3$. The zone of good confinement shrinks with the increase of T_i and spreads otherwise. In our simulations the confinement improves with the increase of B which is clear from the ion transport coefficient. It also increase with P_{NB} due to increase the particle source, caused by NBI, to 50-100% of the total source and

correspondent decrease of the CX loss. Powerful NBI can also induce large fraction of the non inductive current. The resulting current flattening could decrease the ion transport coefficient in the bad confinement zone $\chi_i \sim (q-q_{min})^3$.

The SET model was verified against the single RS discharge #E24715 [9] with I_p/B = 1.2MA/3.4T, P_{NB} = 27 MW. The simulation satisfactory predicts the ion temperature profile and averaged behavior of the electron temperature and density. But the SET model does not describe the transport barriers of T_e and n_e, obtained in the experiment (FIG.6). **The SET model should be modified to describe the ITB in the RS discharges** . This model must be further verified versus the experimental data to determine the limits of its applicability and dependencies for the energy confinement on the global plasma parameters.

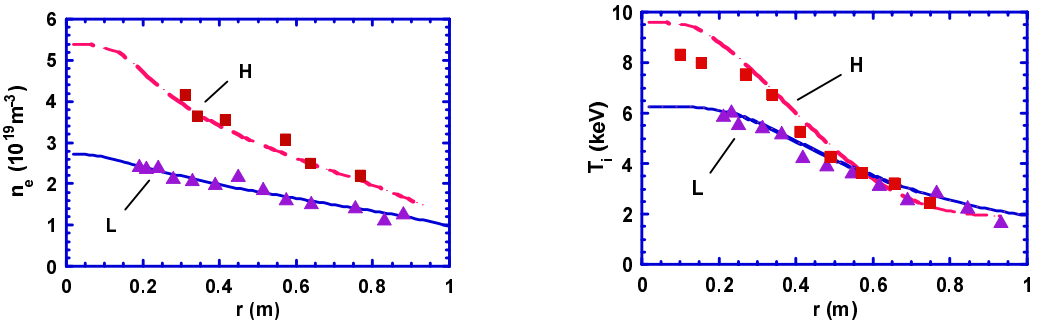

FIG.5. Comparison of the experimental data (dots) with the SETM predictions (curves) for the electron density $n_e(r)$ and ion temperature $T_i(r)$ in the H- and L- mode discharges

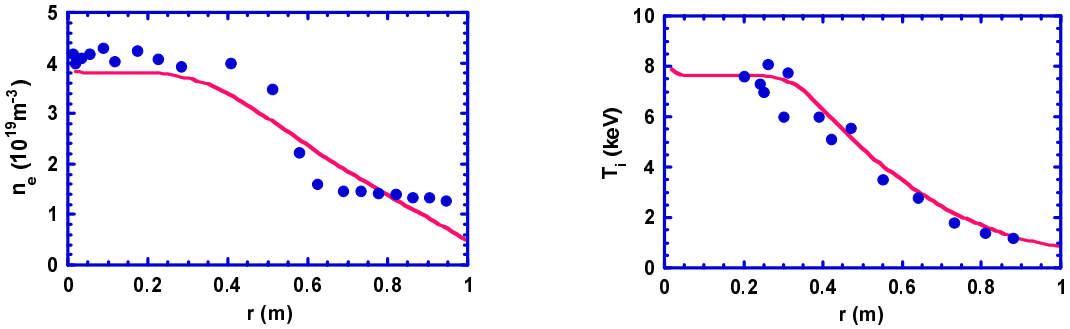

FIG.6. Comparison of the experimental data (dots) with the SETM predictions (curves) for the electron density $n_e(r)$ and ion temperature $T_i(r)$ in the RS discharge #E24715 [9].

ACKNOWLEDGMENTS

We express our gratitude to Dr. M. Azumi and Dr. T. Ozeki for their support of this work.

REFERENCES

[1] KOIDE, Y., et al., Plasma Phys. and Control. Nuclear Fusion Research (Proc. 15th Int. Conf. Seville, 1994), IAEA, Vienna, **1** (1995) 199.
[2] FUJITA, T. et al., Fusion Energy 96 (Proc. 16th Int. Conf. Montreal, 1996), **1** (1997) 227.
[3] DNESTROVSKIJ, Yu.N., et al., Plasma Phys. Reports **23** (1997) 566.
[4] MEREZHKIN,V.G., MUKHOVATOV,V.S., POLEVOI,.A.R. Sov.J.Plasma Phys. **14**(1988) 69.
[5] CONNOR, J. W. and the ITER Confinement Database and Modelling Group, Fusion Energy 96 (Proc 16th Int. Conf., Montreal, 1996) **2** (1997) 935.
[6] POLEVOI, A., SHIRAI, H., TAKIZUKA, T. JAERI-Data/Code 97-014, (1997).
[7] PEREVERZEV, G.V. et. al. Rep. IPP 5/42, Garching, (1991).
[8] GOTT, Yu.V., YURCHENKO, E.I. Plasma Physics Reports, **20** (1994) 853.
[9] FUJITA, T., et. al., Phys. Rev. Letters **12** (1997) 2377.